A Transformerless Solar Network with Eleven Level Grid-Connected Converter

Gudala Satya pratap[1], Kondapalli Paparao[2]
PG Student, Department of EEE, KIET, Kakinada, India.[1]
Asst. Professor, Department of EEE, KIET, Kakinada, India.[2]

***Abstract*— A single-phase transformerless grid-connected photovoltaic converter based on two cascaded full bridges with different dc-link voltages is proposed in this paper. The converter can synthesize up to eleven voltage levels with a single dc bus, since one of the full bridges is supplied by a flying capacitor. The multilevel output decreased the harmonic distortion and electromagnetic interference. A suitable switching strategy is employed to regulate the flying-capacitor voltage, improve the efficiency and minimize the common-mode leakage current with the help of a novel dedicated circuit (transient circuit). Two bidirectional switches are added to the circuit for the required inverter levels. Feasibility performance of the proposed converter is observed by implementing the proposed topology in MATLAB/Simulink environment.**

Index Terms—Leakage current, multilevel systems, photovoltaic (PV) systems, pulsewidth modulation (PWM) inverters.

I. INTRODUCTION

Renewable energy sources like photovoltaic (PV) converters represent the most widespread solution for residential renewable energy generation. The ever-increasing energy consumption, fossil fuels soaring costs and exhaustible nature, and worsening global environment have created a booming interest in renewable energy generation systems, one of which is photovoltaic. Such a system generates electricity by converting the Sun's energy directly into electricity. Photovoltaic-generated energy can be delivered to power system networks through grid-connected inverters. While classical designs of PV converters feature a grid frequency transformer, which is a typically heavy and costly component, at the interface between the converter and the electrical grid, researchers are now considering transformerless architectures in order to reduce costs and weight and improve efficiency. A nine level system is implemented in [1] with a transformerless methodology. Removing the grid frequency transformer entails all the benefits above but worsens the output power quality, allowing the injection of dc current into the grid [2], [3] and giving rise to the problem of ground leakage current [4], [5]. Although the active parts of PV modules might be electrically insulated from the ground-connected mounting frame, a path for ac ground leakage currents generally exists due to a parasitic capacitance between the modules and the frame and to the connection between the neutral wire and the ground, usually realized at the low-voltage/medium-voltage (LV/MV) transformer [3]. Several solutions can be found in literature aiming at the reduction of the common-mode voltage harmonic content [6]–[8]. Once the grid frequency transformer is removed from a PV converter, the bulkiest wound and reactive components that remain are those that form the output filter used to clean the output voltage and current from high frequency switching components. Further reduction in cost and weight and improvement in efficiency can be achieved by reducing the filter size, and this is the goal of multilevel converters. Multilevel converters have been investigated for years [9], but only recently have the results of such researches found their way to commercial PV converters. Since they can synthesize the output voltages using more levels, multilevel converters outperform conventional two- and three-level converters in terms of harmonic distortion. Moreover, multilevel converters subdivide the input voltage among several power devices, allowing for the use of more efficient devices.

Multilevel converters were initially employed in high-voltage industrial and power train applications. They were first introduced in renewable energy converters inside utility-scale plants, in which they are still largely employed [10]–[14]. Recently, they have found their way to residential-scale single-phase PV converters, where they currently represent a hot research topic [15]. Single-phase multilevel converters can be roughly divided into three categories based on design: neutral point clamped (NPC), cascaded full bridge (CFB), and custom. In NPC topologies, the electrical potential between the PV cells and the ground is fixed by connecting the neutral wire of the grid to a constant potential, resulting from a dc-link capacitive divider. A huge advantage is that single-phase NPC converters are virtually immune from ground leakage currents, although the same is not true for three-phase NPC converters [13].

Multilevel inverters are promising; they have nearly sinusoidal output voltage waveforms, output current with better harmonic profile, less stressing of electronic components owing to decreased voltages, switching losses that are lower than those of conventional two-level inverters, a smaller filter size, and lower EMI, all of which make them cheaper, lighter, and more compact. A similar approach is followed in this paper. Moreover, the developed PWM strategy, in addition to controlling the flying capacitor voltage, with the help of the specific TC illustrated in Section IV, minimizes the ground leakage current.

ISSN: 2278 – 7798

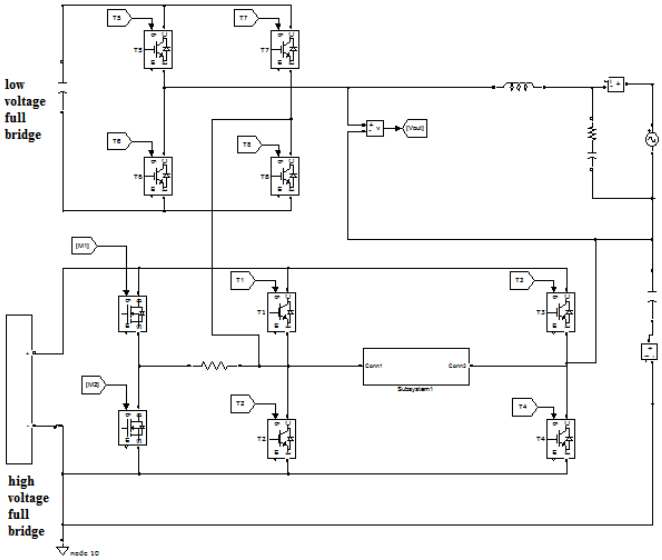

Fig. 1. CFB with a flying capacitor.

Finally, it is important to put in evidence that the proposed converter can work at any power factor as reported in below Section, while not all the alternative proposals can continuously supply reactive power. This paper is organized as follows: Section II presents the power converter topology and the PWM control strategy chosen in order to maximize the performance with the use of a low-cost digital signal processor (DSP). Section III describes the regulation of the flying capacitor used to supply the second full bridge of the CFB topology. Section IV describes the applications if transformerless converters. Section V illustrates the bidirectional switching configuration. Section VI shows the simulation results follows by the conclusion in Section VII.

II. ELEVEN-LEVEL CONVERTER AND PWM CONTROL STRATEGY

The proposed converter is composed of two CFBs, one of which is supplied by a flying capacitor (see Fig. 1). This basic topology was already presented in . In this paper, a different PWM strategy was developed in order to allow grid connected operation with no galvanic isolation (transformerless solution) for this basic topology. Since the PWM strategy alone is not sufficient to maintain a low ground leakage current, other components were added as will be shown in Section IV. As it will be described in the following, the proposed PWM strategy stretches the efficiency by using, for the two legs where PWM frequency switching does not occur, devices with extremely low voltage drop, such as MOSFETs lacking a fast recovery diode. In fact, the low commutation frequency of those two legs allows, even in a reverse conduction state, the conduction in the channel instead of the body diode (i.e., active rectification). Insulated-gate bipolar transistors (IGBTs) with fast anti parallel diodes are required in the legs where high-frequency hard switching commutations occur. In grid-connected operation, one full-bridge leg is directly connected to the grid neutral wire, whereas the phase wire is connected to the converter through an LC filter.

As it will be described and justified in the following section, flying-capacitor voltage Vfc is kept lower, at steady state, than dc-link voltage VDC. Accordingly, the full bridge supplied by the dc link is called the high-voltage full bridge (HVFB), whereas the one with the flying capacitor is the low-voltage full-bridge (LVFB). The CFB topology allows certain degrees of freedom in the control, so that different PWM schemes can be considered; however, the chosen solution needs to satisfy the following requirements.

1) Most commutations must take place in the LVFB to limit the switching losses.

2) The neutral-connected leg of the HVFB needs to switch at grid frequency to reduce the ground leakage current.

3) The redundant states of the converter must be properly used to control the flying-capacitor voltage.

4) The driving signals must be obtained from a single carrier for a low-cost DSP to be used as a controller.

The switching pattern was developed starting from the above requirements. Requirement 2), in particular, is due to the aforementioned parasitic capacitive coupling between the PV panels and their frames, usually connected to the earth. Capacitive coupling renders the common-mode current inversely proportional to the switching frequency of the neutral-connected leg. The converter can operate in different output voltage zones, where the output voltage switches between two specific levels.

The operating zone boundaries vary according to the dc-link and flying-capacitor voltages, and adjacent zones can overlap (see Fig. 2). In zones labeled A, the contribution of the flying-capacitor voltage to the converter output voltage is positive, whereas it is negative in B zones. Constructive cascading of the two full bridges can, therefore, result in limited output voltage boosting. Depending on the V_{fc}/V_{DC} ratio, one of the (a) or (b) situations in Fig. 2 can ensue; nevertheless, the operation of the converter does not differ much in the two cases. If two overlapping operating zones can supply the same output voltage, the operating zone to be used is determined taking into account the regulation of V_{fc}, as will be described in Section III. The switching pattern depends on the instantaneous fundamental component of output voltage V^*_{out} and on the measured values of V_{fc} and VDC.

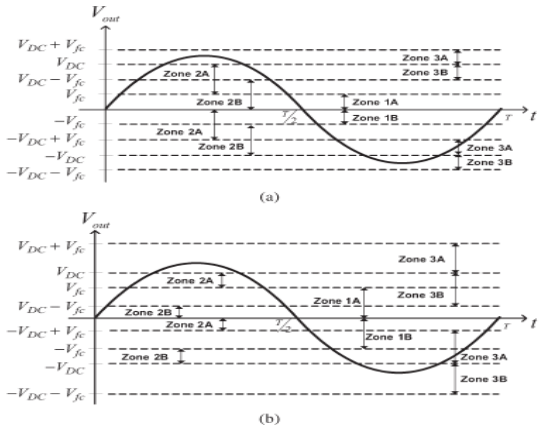

Fig. 2. Operating zones under different *V*fc ranges.
(a) *V*fc < 0.5*V*DC.
(b) *V*fc > 0.5*V*DC.

ISSN: 2278 – 7798

If $V_{fc} = V_{DC}/3$, the converter can synthesize eleven equally spaced output voltage levels. Moreover, apart from zone 2, no high-frequency commutations occur in the whole HVFB (see Fig. 2). Since the voltage regulation of the flying capacitor takes place in zone 2, the zone-2 behavior is more articulated and will be described in detail in the following section.

III. Flying-Capacitor Voltage Regulation

Since the main task facing a grid-connected PV converter is the transfer of active power to the electrical grid, controlling the voltage of the flying capacitor is critical. Flying-capacitor voltage V_{fc} is regulated by suitably choosing the operating zone of the converter depending on the instantaneous output voltage request. Depending on the operating zone of the converter (see Fig. 2), V_{fc} can be added to (A zones) or subtracted from (B zones) the HVFB output voltage, charging or discharging the flying capacitor. In particular, considering a positive value of the current injected into the grid, the flying capacitor is discharged in A zones and charged in B zones. Since a number of redundant switch configurations can be used to synthesize the same output voltage waveform, it is possible to control the voltage of the flying capacitor, forcing the converter to operate more in A zones when the flying-capacitor voltage is higher than a reference value or more in B zones when it is lower than a reference value. Similar considerations hold in case of a negative injected grid current. In each case, some commutations between nonadjacent output Levels must inevitably occur (level skipping), with the drawback of a certain increase in the output current ripple. The voltage control of the flying capacitor (which determines the zone-A or zone-B operation) is realized by a simple hysteresis control.

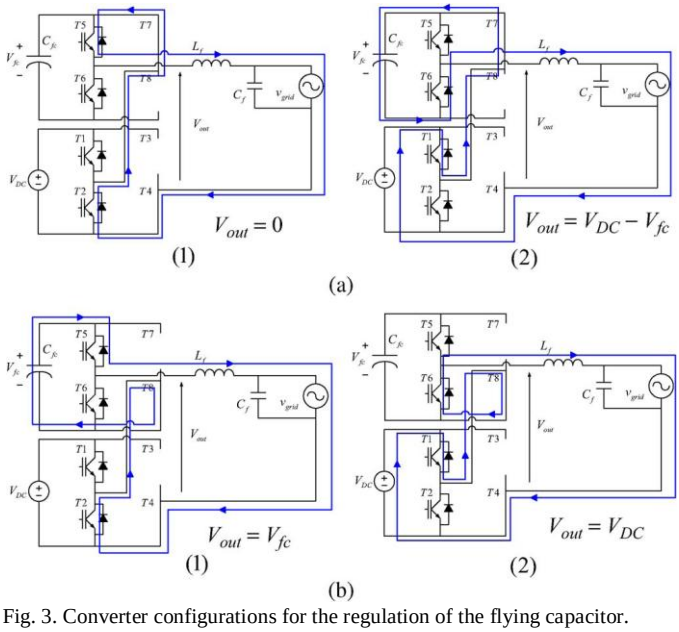

Fig. 3. Converter configurations for the regulation of the flying capacitor.
(a) Flying-capacitor charge.
(b) Flying-capacitor discharge.

Fig. 3 illustrates the regulation of Vfc supposing a positive grid current with $V_{out} > 0$ and $V_{fc} < 0.5V_{DC}$. If V_{fc} is too low, output level V_{fc} can be replaced by $V_{DC} - V_{fc}$, thus switching between the 0 and $V_{DC} - V_{fc}$ output levels [zone 2B, Fig. 4(a)]. Similarly, if V_{fc} is too high, $V_{DC} - V_{fc}$ can be replaced with V_{fc}, causing the converter to switch between the V_{fc} and V_{DC} output levels [zone 2A, Fig. 3(b)]. In Fig. 4, the devices switching at low frequency are short circuited when on and not shown when off. Similar V_{fc} regulation strategies can be likewise developed for the case when $V_{fc} > 0.5V_{DC}$.

If $V_{fc} < 0.5V_{DC}$, in order to minimize the current ripple, zone 2 is chosen only when $V_{fc} < V^*out < V_{DC} - V_{fc}$ (zones 3 are otherwise chosen), limiting level skipping. Level skipping always occurs if $V_{fc} > 0.5V_{DC}$; hence, any A or B zone can be chosen according to the voltage regulation algorithm. Since the dc-link voltage can go through sudden variations due to the MPPT strategy, it is important that the converter is able to work in any [V_{DC}, V_{fc}] condition. While the distortion of the output voltage is minimized through the on-line duty cycle computation, it is important to assess the capability of the converter to regulate the flying-capacitor voltage under different operating conditions. The ability to control the flying-capacitor voltage through the proposed PWM strategy has been studied in simulation by determining the average flying-capacitor current under a large span of V_{DC} and V_{fc} values. In the simulations, grid voltage vgrid is sinusoidal with an amplitude of 230 $\sqrt{2}$ V; however, the same results hold even for different voltages if the ratio V_{grid}/V_{DC} remains constant.

IV. Transformerless PV Converters

The commutation pattern provides T3 and T4 switch at grid frequency, commutating at every zero crossing of v_{grid}. If the zero crossing with a negative derivative is considered, T4 opens and T3 closes, changing the neutral wire voltage (and thus the voltage across the parasitic capacitance of the PV field) from zero to VDC.. A proper TC was designed to decrease these surge currents. Fig. 3(a) shows the proposed converter topology; it is constituted of the two-cell CFB described in Fig. 1 with the addition of the TC components. In order to better understand the behavior of the TC, the distributed parasitic capacitance of the PV source was modeled with a simple equivalent parasitic capacitance, i.e., Cp, connected between the negative pole of the dc link and the ground.

The TC consists of two low-power MOSFETs M1, and M2, resistor RT, bidirectional switch T9. When the converter enters operating zone 1, the HVFB output voltage must be zero, obtained by switching T1 and T3 or T2 and T4 on. Nevertheless, to operate the TC, when entering zone 1, T1, T2, T3, and T4 are all kept off, while T9 is on. This keeps the neutral potential floating, so that the voltage on the parasitic capacitor V_{ground} stays constant . At this point, one of M1 and M2 is turned on (M1 if the slope of the zero crossing is negative and M2 if positive). So doing, C_p is charged through R_T with a first-order transient [see Fig. 4(b)], limiting the current surge.

ISSN: 2278 – 7798

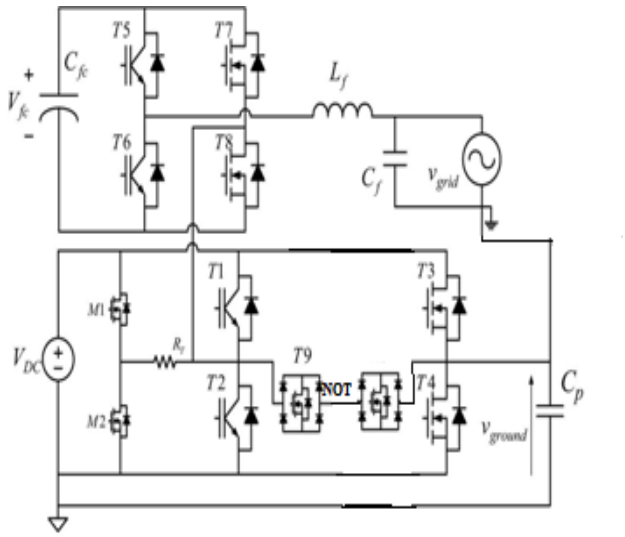

(a)

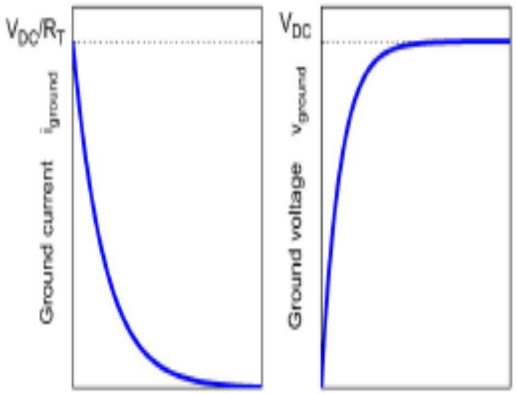

(b)

Fig. 4. Ground leakage current limitation circuit topology and behavior. (a) TC topology. (b) TC waveforms.

Whereas the TC introduces additional components, they can be selected with current ratings much lower than the devices of the CFB. Moreover, the power loss due to the added resistor is negligible. Estimating the energy lost charging and discharging a capacitor C_p to V_{DC} averaged over a line period T by $P_{tc} = C_p V^2_{DC}/T$, with C_p = 200 nF and V_{DC} = 300 V, a dissipation of about 1Wis obtained. The operation of the TC is not affected by the power factor because in grid-connected operation, the output voltage is always very close to the grid voltage. The correct operation of the TC requires the grid voltage instantaneous angle that can be obtained with a phase-locked loop (PLL) fed by the grid voltage.

V. BIDIRECTIONAL SWITCHING CONFIGURATION

The Fig 5 shows the bilateral switch configuration, here we can see T9 is connected to two bidirectional switches with NOT gate. This means either of the switches will operate at a time.

In [1] single bidirectional switch is used for nine level output, but here we implemented two switch topology for increasing the output level. By increasing the number of cascaded H-bridges, the number of levels in CHB inverters increases. Generally if the number of output voltage levels is increased, then the number of power electronic devices and the number of isolated DC sources is also increased. This makes a CHB inverter further complex. In this paper, a novel multilevel inverter with minimum number of power electronic switching devices is proposed which is a modified version of the multilevel inverter. The proposed Multilevel Inverter Bridge carries an two auxiliary switches which will be Bi-directional in nature.

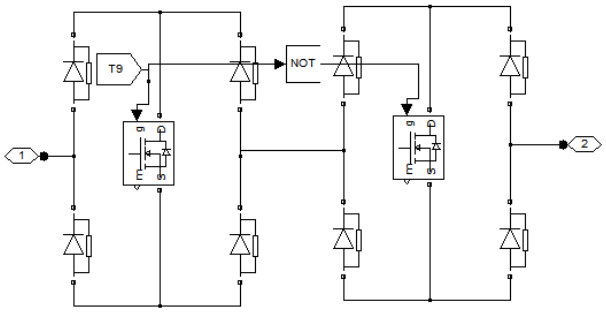

Fig. 5. Bidirectional switch configuration

The proposed multilevel inverter topology can be extended for the application of grid connected photo voltaic systems, hybrid electric vehicles, etc. Furthermore, simulation results are also presented to demonstrate the validity of the proposed single phase multilevel inverter. Basically Inverter is a device that converts DC power to AC power at desired output voltage and frequency. Demerits of inverter are less efficiency, high cost, and high switching losses. To overcome these demerits, we are going to multilevel inverter. The term Multilevel began with the three-level converter. The concept of multilevel converters has been introduced and the cascade multilevel inverter was first proposed in 1975. In recent years multi level inverters are used high power and high voltage applications. Multilevel inverter output voltage produce a staircase output waveform, this waveform look like a sinusoidal waveform. The multilevel inverter output voltage having less number of harmonics compare to the conventional bipolar inverter output voltage. If the multilevel inverter output increase to N level, the harmonics reduced to the output voltage value to zero. That is why we simply implemented a two bidirectional switch configuration to increase the level of inverter without adding bridges to the circuit.

VI. SIMULATION RESULTS

The proposed converter and PWM were extensively simulated under MATLAB/Simulink. The simulations cover a large range of active and reactive power injected into the grid, dc-link voltage, and equivalent PV parasitic capacitance. A dc-link voltage VDC = 300 V was used in the simulations, unless otherwise specified. The grid was represented by a sinusoidal voltage source at 50 Hz of amplitude v_{grid} = 230 V. The output filter was composed of a capacitor Cf = 1 μF and an inductor Lf = 1.5 mH. An additional inductor L_{grid} = 40 μH represented the total distributed grid inductance. The PWM frequency was fs = 20 kHz, and the flying capacitor had a

ISSN: 2278 – 7798

capacitance of C_{fc} = 500 µF. The surge limiting resistance RT was selected as 1.5 kΩ. The current injected into the grid was regulated through a proportional-integral regulator plus feedforward at i_{grid} = 8.5 A rms. As stated above, the injection of both active and reactive power was simulated; however, the switches being ideal and the commutations instantaneous, performance did not depend on the power factor. For this reason, only the unity power factor simulation results are reported. In the simulations, the grid voltage angle information is available; hence, a PLL was not employed.

Fig. 6 shows the output voltage and current under different conditions of the dc voltage ratio. As expected, the THD of the grid current increases with the dc voltage ratio, being 2.7%, 3%, and 3.3%, respectively, for V_{fc}/V_{DC} = 0.33, V_{fc}/V_{DC} = 0.5, and V_{fc}/V_{DC} = 0.66. Fig. 7 shows the performance of the TC with a parasitic capacitance of the PV field of Cp = 200 nF. The ground leakage current results i_{ground} = 30 mA rms. Please note that only a common-mode inductor of 1 mH was employed in this setup. The ground leakage current could be further reduced by a more accurate design of the common-mode filter. In order to obtain further indications about the regulation of the flying-capacitor voltage, Fig. 8 reports the result of a step variation of V_{fc} from 150 to 190 V (inside the controllable region in Fig. 4) occurring at time 0.1 s. As it can be seen, the average value of V_{fc} rapidly (in about 25 ms) rises to the reference value without any overshoot.

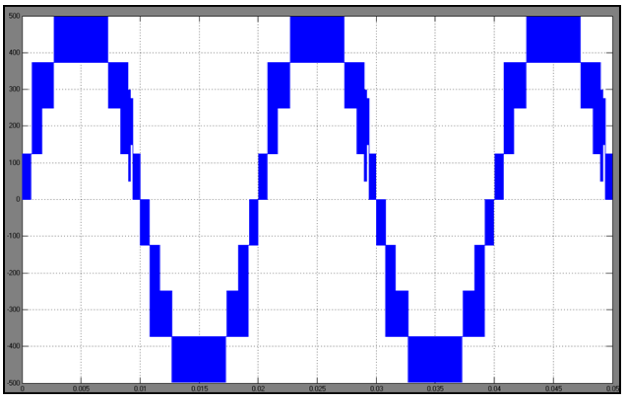

(a)

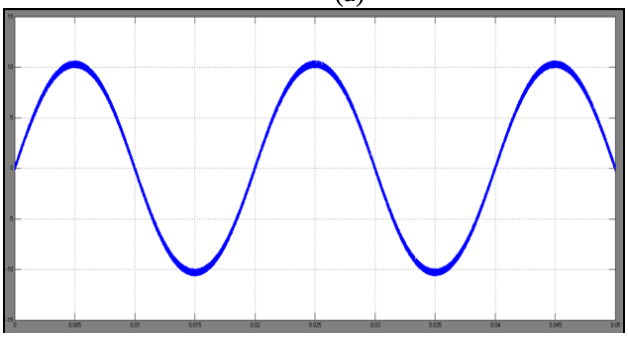

(b)

V_{fc}/V_{DC} = 0.33,

Fig. 6. Simulation results of eleven level voltage (a) and current (b) with V_{DC} = 300 V.

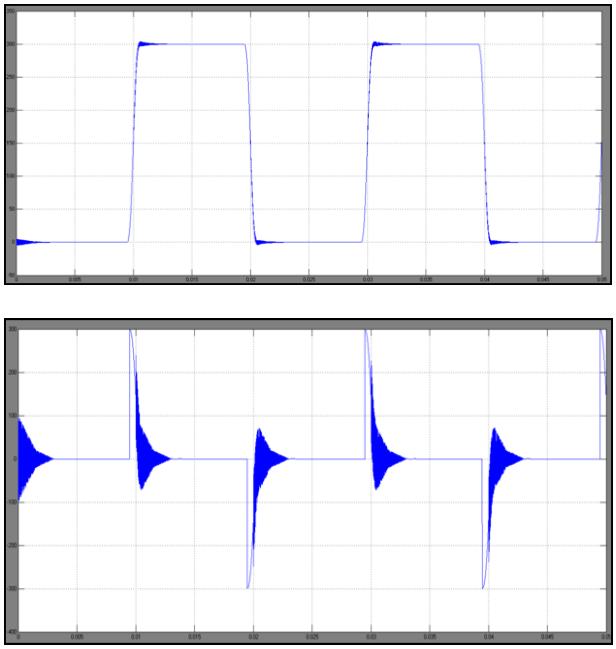

Fig. 7. TC behavior with a 200 nF parasitic capacitor.

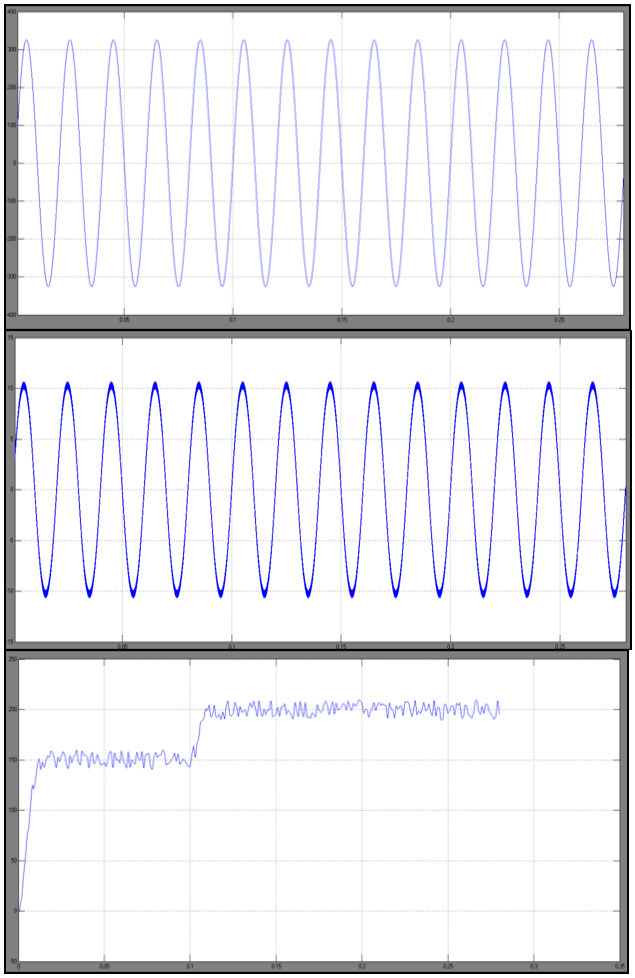

Fig. 8. V_{fc} step variation response.

ISSN: 2278 – 7798

VII. Conclusion

A novel Eleven-level grid-connected transformerless PV converter based on a CFB topology with two full bridges, one of which is supplied by a floating capacitor and another with a dc source. A suitable PWM strategy was developed in order to improve efficiency and, with the help of a specific TC, minimize the ground leakage current. The proposed PWM strategy can regulate the voltage across the flying capacitor. Simulations were performed to assess the ability to regulate the flying-capacitor voltage in a wide range of operating conditions. Extensive simulations and results shows the good performance of the converter as far as ground leakage current and harmonic distortion are concerned. This proposed converter with two bidirectional switches can continuously operate at arbitrary power factors, has limited boosting capability, and can produce eleven output voltage levels with 12 power switches, of which three are low power switches for the TC and only four need to be controlled by PWM.

References

[1]. Giampaolo Buticchi, Davide Barater, and E.Lorenzani, "A Nine-Level Grid-Connected Converter topology for Single-Phase Transformerless PV Systems," IEEE Trans.Ind. Electron., vol. 61, no. 8, pp. 3951–3960, Aug. 2014.

[2]. G. Buticchi, L. Consolini, and E. Lorenzani, "Active filter for the removal of the dc current component for single-phase power lines," IEEE Trans.Ind. Electron., vol. 60, no. 10, pp. 4403–4414, Oct. 2013.

[3]. G. Buticchi and E. Lorenzani, "Detection method of the dc bias in distribution power transformers," IEEE Trans. Ind. Electron., vol. 60, no. 8, pp. 3539–3549, Aug. 2013.

[4]. H. Xiao and S. Xie, "Leakage current analytical model and application in single-phase transformerless photovoltaic grid-connected inverter," IEEE Trans. Electromagn. Compat., vol. 52, no. 4, pp. 902–913, Nov. 2010.

[5]. O. Lopez, F. Freijedo, A. Yepes, P. Fernandez-Comesaa, J. Malvar, R. Teodorescu, and J. Doval-Gandoy, "Eliminating ground current in a transformerless photovoltaic application," IEEE Trans. Energy Convers., vol. 25, no. 1, pp. 140–147, Mar. 2010.

[6]. S. Araujo, P. Zacharias, and R. Mallwitz, "Highly efficient single-phase transformerless inverters for grid-connected photovoltaic systems," IEEE Trans. Ind. Electron., vol. 57, no. 9, pp. 3118–3128, Sep. 2010.

[7]. D. Barater, G. Buticchi, A. Crinto, G. Franceschini, and E. Lorenzani, "Unipolar PWM strategy for transformerless PV grid-connected converters," IEEE Trans. Energy Convers., vol. 27, no. 4, pp. 835–843, Dec. 2012.

[8]. T. Kerekes, R. Teodorescu, P. Rodridguez, G. Vazquez, and E. Aldabas, "A new high-efficiency single-phase transformerless PV inverter topology,"IEEE Trans. Ind. Electron., vol. 58, no. 1, pp. 184–191, Jan. 2011.

[9]. S. Kouro, M. Malinowski, K. Gopakumar, J. Pou, L. Franquelo, B. Wu, J. Rodriguez, M. P. Andrez, and J. Leon, "Recent advances and industrial applications of multilevel converters," IEEE Trans. Ind. Electron., vol. 57, no. 8, pp. 2553–2580, Aug. 2010.

[10]. Y. Xue, B. Ge, and F. Z. Peng, "Reliability, efficiency, and cost comparisons of mw-scale photovoltaic inverters," in Proc. IEEE ECCE, Raleigh, NC, USA, Sep. 2012, pp. 1627–1634.

[11]. C. Townsend, T. Summers, and R. Betz, "Control and modulation scheme for a cascaded H-bridge multi-level converter in large scale photovoltaic systems," in Proc. IEEE ECCE, Raleigh, NC, USA, Sep. 2012, pp. 3707–3714.

[12]. S. Essakiappan, H. Krishnamoorthy, P. Enjeti, R. Balog, and S. Ahmed, "Independent control of series connected utility scale multilevel photovoltaic inverters," in Proc. IEEE ECCE, Raleigh, NC, USA, Sep. 2012, pp. 1760–1766.

[13]. G. Konstantinou, S. Pulikanti, M. Ciobotaru, V. Agelidis, and K. Muttaqi, "The seven-level flying capacitor based ANPC converter for grid integration of utility-scale PV systems," in Proc. IEEE PEDG, Aalborg, Denmark, Jun. 2012, pp. 592–597.

[14]. G. Brando, A. Dannier, A. Del Pizzo, and R. Rizzo, "A high performance control technique of power electronic transformers in medium voltage grid-connected PV plants," in Proc. ICEM, Rome, Italy, Sep. 2010, vol. 2, pp. 1–6.

[15]. G. Buticchi, E. Lorenzani, and G. Franceschini, "A five-level single-phase grid-connected converter for renewable distributed systems," IEEE Trans. Ind. Electron., vol. 60, no. 3, pp. 906–918, Mar. 2013.

[16]. Y. Kashihara and J. Itoh, "The performance of the multilevel converter topologies for PV inverter," in Proc. CIPS, Beijing, China, Mar. 2012, pp. 1–6.

ISSN: 2278 – 7798